Received: 15 November 2019 | Revised: 23 January 2020 | Accepted: 13 February 2020

DOI: 10.1002/qua.26203

FULL PAPER

International Journal of Quantum Chemistry WILEY

Electron correlation effects in cobalt fluorides CoF_n

Christian Stemmle | Beate Paulus

Institut für Chemie und Biochemie - Arnimallee 22, Freie Universität Berlin, Berlin, Germany

Correspondence
Christian Stemmle, Institut für Chemie und Biochemie - Arnimallee 22, 14195 Berlin, Freie Universität Berlin, Germany.
Email: christian.stemmle@fu-berlin.de

Funding information
Deutsche Forschungsgemeinschaft, Grant/Award Numbers: SFB 1349 Fluorine-Specific Interactions, 387284271

Abstract

The molecular cobalt fluorides CoF_2, CoF_3 and CoF_4 are studied and compared by employing different basis sets as well as Quantum Information Theory (QIT) to investigate their correlation effects. These prototypical monomers may be systematically extended in size yielding a novel quasi 1-dimensional, strongly correlated model system consisting of cobalt atoms bridged by oxygen atoms and fluorine termination on both ends. Accurate correlation energies are obtained using Full Configuration Interaction (FCI) and Full Configuration Interaction Quantum Monte Carlo (FCIQMC) calculations and the results are compared to Coupled Cluster and Density Matrix Renormalization Group (DMRG) energies. The analysis indicates the cobalt atom requires a larger number of one-electron basis functions than fluorine and the use of localized molecular orbitals may facilitate calculations for the extended systems.

KEYWORDS

correlation effects, electronic structure, orbital entanglement, strong correlation

1 | INTRODUCTION

Accurate treatment of electron correlation is the main challenge in electronic structure theory. Electron correlation describes the difference between the Hartree-Fock (HF) solution, which represents a systematic approximation to solve the electronic Schrödinger equation, and the exact solution. HF relies on an ansatz for the wave function that is only exact for a system with noninteracting electrons, the Slater determinant. The family of wave function-based correlation methods provides an approach capable of resolving this error in the numerically exact limit of the employed one-electron basis set, known as the full configuration interaction (FCI) method.[1] Unfortunately it scales exponentially with the number of electrons and basis functions that limits practical application to very small systems with only a few electrons.

One therefore tries to reduce the high computational cost by considering the largest contributions (electron configurations) only. *A priori* knowledge of which configurations to keep however is hard and only possible based on assumptions. As a consequence, a large number of different truncation schemes and methods have been developed, such as CCSD(T),[2,3] MRCI,[4] CASSCF,[4,5] DMRG,[6] FCIQMC,[7] and so on. An especially difficult class of problems are *strongly* correlated systems where partially occupied, near degenerate orbitals are present. This leads to multiple major configurations with similar weight and, due to the truncation of the FCI wave function, a balanced description of the orbitals with respect to all major configurations is required.

Typical test systems to evaluate newly developed methods range from more abstract systems like the Hubbard model[8] over chains and lattices of hydrogen atoms[9,10] to small but realistic chemical systems like the dissociation of N_2[7,11] or transition metal complexes.[12] We here propose a new system based on cobalt compounds that may be systematically extended in size. The prototypical "monomers" CoF_2 and CoF_4 (in its quadratic planar geometry D_{4h}) are high-spin complexes, and thus feature a large number of unpaired electrons. The systems may be systematically enlarged by forming linear chains where Co atoms are bridged with oxygen atoms, as depicted in Figure 1. The planar $Co^{IV}O_2$ chains have indeed been experimentally prepared and studied on Ir (100) surfaces[13,14] and showed ferromagnetic properties.

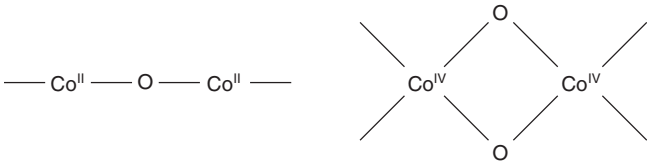

FIGURE 1 Structures for linear chains of $Co^{II}O$ and $Co^{IV}O_2$. The chains may be arbitrarily extended and terminated with fluorine

As the longer chains require the treatment of many (unpaired) electrons we here start by investigating the monomers CoF_2 and CoF_4, as well as the intermediate CoF_3. The ground state structure of CoF_4 has a tetrahedral (T_d) geometry and is therefore considered as well. The three compounds CoF_2, CoF_3, and CoF_4 (T_d) have been identified experimentally by matrix-isolated IR spectroscopy[15] and mass spectrometric data of the cationic species is available as well.[15,16] Theoretical studies on the CCSD(T)/aVTZ and B3LYP/aVTZ levels of theory[17] confirm the high-spin character and show that CoF_4 and CoF_3 are thermodynamically stable under the release of F or F_2.[17] The minimum structures are found to be linear ($D_{\infty h}$) for CoF_2,[17,18] trigonal planar (D_{3h}) for CoF_3,[17,19,20] and tetrahedral (T_d) for CoF_4.[17]

A practical application of the compounds is the Fowler process,[21] the synthesis of fluorocarbons by reduction of CoF_3 to CoF_2. The trifluoride is later regenerated by fluorination of CoF_2 with F_2. Similar, molecular CoF_4 is of potential interest as an oxidation or fluorination reagent, as it constitutes the highest neutral cobalt fluoride.[16,22]

The four model systems will be investigated by systematic variation of the one-electron basis set. Accurate correlation energies are obtained by conventional FCI or full configuration interaction quantum Monte Carlo (FCIQMC), depending on the basis set size. Additionally, density matrix renormalization group (DMRG) calculations and subsequent quantum information theory (QIT) analysis[23] are applied.

2 | THEORY

2.1 | Density matrix renormalization group and quantum information theory

Originally invented by White,[6] the DMRG method is especially suited to treat strong correlations in large active spaces and closely connected to QIT.[23] The latter allows for a quantitative analysis of the correlation (entanglement) effects of either individual or groups of orbitals. Both, DMRG and QIT, are described in detail in various reviews,[12,24–29] therefore only a brief overview is given here.

In DMRG the electronic wave function $|\Psi\rangle$ is represented by the d-order tensor U containing the configuration interaction (CI) coefficients, where d is the number of orbitals. This tensor is then factorized into a matrix product state (MPS), where each (spatial) orbital i is represented by a matrix A_i.

$$|\Psi\rangle = \sum_{\alpha_1,\ldots,\alpha_d} U(\alpha_1,\ldots,\alpha_d)\,|\phi_{\alpha_1}^{\{1\}}\rangle\otimes\ldots\otimes|\phi_{\alpha_d}^{\{d\}}\rangle \tag{1}$$

$$U(\alpha_1,\ldots,\alpha_d) = A_1(\alpha_1)A_2(\alpha_2)\cdots A_{d-1}(\alpha_{d-1})A_d(\alpha_d) \tag{2}$$

The indices α_i label the four possible occupations of each spatial orbital, that is, the single-orbital basis states $|\phi_{\alpha_i}^{\{i\}}\rangle$. The orbitals are considered to be arranged on a chain and the corresponding matrices are connected to their neighbors by a virtual index. Contraction (multiplication) of two matrices along their shared virtual index creates a combined subsystem. Contraction of all matrices A_i recovers the full wave function. Numerical accuracy can be controlled by the number of blockstates M, which truncates each virtual index to its M largest contributions. The lower limit $M = 1$ recovers the HF solution and leads to small matrices, that is, low memory requirements. In the numeric exact limit $M \to \infty$ the FCI results are obtained. Alternatively, the accuracy can be adaptively controlled by the dynamic block state selection (DBSS) approach,[30,31] where the number of blockstates is chosen such that a user-defined truncation error for the density matrix is not exceeded. In the DMRG algorithm, an effective Hamiltonian for a subset of orbitals (typically two) is formed by contracting the MPS with the Hamiltonian over all except the selected orbitals. Diagonalization and factorization of the obtained eigenvector into the selected orbitals then leads to an updated set of matrices A_i. This process is then iteratively repeated while sweeping forward and backward through the chain of orbitals until convergence is achieved. The CI problem is thus solved by diagonalizing many small, effective Hamiltonians instead of one large Hamiltonian.

QIT relies on the n-orbital reduced density matrices that are obtained by tracing over all but n orbital indices, for example, the 1-orbital reduced density matrix is given by

$$\rho_i(\alpha_i,\alpha_i') = \mathrm{Tr}_{1,\ldots,\not{i},\ldots,d}\,|\Psi\rangle\langle\Psi| \tag{3}$$

$$= \sum_{\alpha_1,\ldots,\not{\alpha_i},\ldots,\alpha_d} U(\alpha_1,\ldots,\alpha_i,\ldots,\alpha_d)\overline{U(\alpha_1,\ldots,\alpha_i',\ldots,\alpha_d)}. \tag{4}$$

and can be directly obtained from contraction of the MPS. The n-orbital reduced density matrix then encodes the entanglement of the subsystem of n orbitals with its environment. This may be quantified by calculating the von Neumann entropy[32] of all eigenvalues $\omega_{i,\alpha}$. For example the 1-orbital entropy of orbital i is defined as

$$S_i = -\mathrm{Tr}(\rho_i \ln \rho_i) = -\sum_{\alpha} \omega_{i,\alpha} \ln \omega_{i,\alpha}. \tag{5}$$

Large values of S_i indicate large entanglement, while values close to zero represent negligible entanglement of the corresponding orbital. Similar, the 2-orbital entropy S_{ij} describes the amount of entanglement between both combined orbitals and the environment. But it does not include any entanglement between i and j, which may therefore be recovered as the difference between the 2-orbital entropy and both 1-orbital entropies. This is called the mutual information I_{ij}.

$$I_{ij} = S_i + S_j - S_{ij} \tag{6}$$

Additionally, the so-called total correlation

$$I_{\mathrm{tot}} = \sum_i S_i \tag{7}$$

can be considered. On a side note, we would like to mention that the name total *correlation* might be misleading in the context of this work. A more intuitive name might be total *entropy* or total *entanglement*. However we will stick with the name established in previous literature.

2.2 | Full configuration interaction quantum Monte Carlo

The FCIQMC was recently introduced by Booth et al.[7] It combines the expansion of the electronic wave function in determinants from FCI with the propagation of random walkers from Quantum Monte Carlo. If the walker population is at equilibrium, then the number of walkers N_i on each determinant $|i\rangle$ is proportional to its CI coefficients C_i

$$C_i \propto N_i. \tag{8}$$

The population dynamics is controlled by the coupling between two determinants $|i\rangle$ and $|j\rangle$, given by the Hamiltonian $\hat{H}$.

$$K_{ij} = \langle i|\hat{H}|j\rangle - E_{\mathrm{HF}}\delta_{ij} \tag{9}$$

Together with the imaginary-time Schrödinger equation

$$\frac{\partial \Psi}{\partial \tau} = -\hat{H}\Psi, \tag{10}$$

where $\tau = it$, this yields a set of coupled differential equations

$$-\frac{\mathrm{d}c_i}{\mathrm{d}\tau} = (K_{ii} - S)C_i + \sum_{j \neq i} K_{ij} c_j. \tag{11}$$

Here the parameter S is introduced to control the total number of walkers

$$N_w = \sum_i |N_i| \tag{12}$$

as described below.

After choosing an initial walker population, a three-step algorithm propagates the walker population. The first *spawning* step considers off-diagonal spawning events from a parent determinant i on a child determinant j. With a certain probability depending on the coupling matrix K_{ij}, a

new walker will be spawned. In the second step, diagonal *death/cloning* events will occur on each parent determinant, again with a certain probability. Finally all walkers from the previous two steps are summed on each determinant in the *annihilation* step, that is, walkers with opposite sign on the same determinant cancel out. In the long time limit, this algorithm will eventually equilibrate and oscillate about that equilibrium.

As the walkers on each determinant relate to the CI coefficients, the correlation energy may be obtained from the equilibrated population. Different energy measures exist however. The first one is the energy shift S introduced in Equation (11), which is defined such that it reaches the correlation energy if the walker population remains constant. In practice, S will oscillate around the correlation energy, that is, may be averaged if one continues to sample the equilibrated population. Another measure is the projected energy

$$E(\tau) = \frac{\langle \mathrm{HF}|\hat{H}e^{-\tau\hat{H}}|\mathrm{HF}\rangle}{\langle \mathrm{HF}|e^{-\tau\hat{H}}|\mathrm{HF}\rangle} \tag{13}$$

which may be rearranged to

$$E(\tau) = E_{\mathrm{HF}} + \sum_{j\in\{\mathrm{singles,doubles}\}} \langle j|\hat{H}|\mathrm{HF}\rangle \frac{N_j(\tau)}{N_{\mathrm{HF}}(\tau)}. \tag{14}$$

The power of FCIQMC lies in the number of required walkers. Although a system-dependent number of critical walkers is required to reach a converged energy, this number is much smaller than the number of configurations a deterministic FCI calculation requires. The reason is that although not all determinants are populated by walkers in a certain population snapshot, they still remain accessible in the next iteration. Their effect on all other determinants (spawning of new walkers) can thus be sampled over time.

Typically, a FCIQMC calculation starts with a number of walkers on the HF configuration. The energy shift is then kept constant (eg, $S = 0$) and causes the total number of walkers to grow. Once a user-defined amount of walkers is reached, the calculation switches to constant N_w mode and varies S which allows the walker population to equilibrate.

Two extensions to FCIQMC are the exact deterministic treatment of the most important determinants (semi-stochastic) to reduce the statistical error (noise)[33,34] and the initiator method,[35,36] where only determinants selected as an initiator may spawn walkers on previously unoccupied determinants. This makes the propagation more stable with respect to the number of walkers required. A further extension introduces superinitiators,[37] which marks all populations spawned from a superinitiator as a regular initiator.

3 | COMPUTATIONAL DETAILS

For the CoF_2 molecule, the electronic ground state is reported to be an $^4\Delta_g$ state and the first excited state $^4\Sigma_g^-$ is only about 5 mE_h higher in energy.[18] Due to the reduction to the abelian group D_{2h} the two degenerate $^4\Delta_g$ fall into the A_g and B_{1g} irreducible representations (IRREP), while $^4\Sigma_g^-$ is B_{1g}. The electronic states and the energetic order of the Co 3d orbitals are summarized in Figure 2. For simplicity we will focus on the A_g component of the $^4\Delta_g$ ground state. However, it proved advantageous to optimize the molecular orbitals (MOs) on the CASSCF(7,5) level and include both electronic states in the state averaging procedure. On this level, the $^4\Sigma_g^-$ state is actually lower in energy than the $^4\Delta_g$ ground state. This, however, may be corrected using the higher levels of theory. The electronic, nondegenerate ground states for the other three models are in the total symmetric IRREP and orbitals are based on Restricted Open-Shell Hartree-Fock calculations. All FCI and DMRG calculations exclude core orbitals with eigenvalue below -3 E_h (i.e. 1s, 2s, 2p, 3s, 3p on Co and 1s on F) but keep all virtual orbitals.

The four systems of interest are investigated by a systematic variation of the one-electron basis sets and FCI calculations, ranging from a minimal basis set up to cc-pVDZ[38] on all atoms. The MOs and FCI energies are obtained with the Molpro[39–42] software package. Where a conventional FCI is not possible due to the basis set size, FCIQMC[7] calculations are performed instead. FCIQMC calculations are first equilibrated using

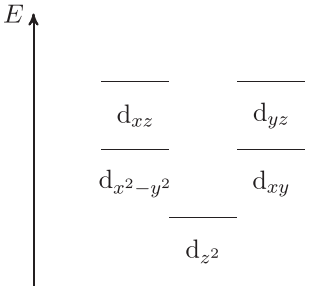

d_{z^2}	$d_{x^2-y^2}$	d_{xy}	d_{xz}	d_{yz}	c_i	
↓↑	↓↑	↑	↑	↑	1.00	$^4\Delta_g\ (A_g)$
↓↑	↑	↓↑	↑	↑	1.00	$^4\Delta_g\ (B_{1g})$
↑	↓↑	↓↑	↑	↑	0.82	$^4\Sigma_g\ (B_{1g})$
↑	↑	↑	↓↑	↓↑	−0.57	$^4\Sigma_g\ (B_{1g})$

FIGURE 2 The Co 3d orbitals in the CASSCF(7,5) calculation of CoF_2 using the cc-pVDZ basis set. The energetic order is plotted to the left. The occupation patterns and CI coefficients c_i of all possible configurations and their corresponding electronic states are indicated to the right

1×10^6 walkers and are then stepwise increased to 1×10^7 and 1×10^8 walkers. Afterward the number of superinitiators is stepwise increased until the averaged correlation energy converges within a user-defined threshold (2×10^{-3} E_h).

The chosen basis sets start with a minimal basis set based on cc-pVDZ on all atoms and then includes stepwise additional atomic orbital (AO) basis functions on the cobalt center, while the fluorine basis set is kept minimal. The largest basis set considers the full cc-pVDZ basis set on all atoms. Detailed information on all used basis sets is available in Tables S1 to S6. Furthermore, the model systems are investigated by DMRG calculations, using a density matrix cutoff for the DBSS approach of 1×10^{-5} and an additional cutoff M_{max} = 1024 for the maximum number of blockstates at each step. DMRG calculations and subsequent QIT analysis are performed using the DMRG Budapest code.[43]

4 | RESULTS AND DISCUSSION

The correlation energies for the isolated ions at different basis sets are summarized in Table 1. Be aware that the fluoride F^- at a minimal basis set does not have any correlation energy. The results are used to determine the amount of correlation energy that arises from combining the atoms in CoF_n by defining the interatomic correlation energy

$$\Delta E_{corr} = E_{corr}(CoF_n) - E_{corr}\left(Co^{n+}\right) - nE_{corr}(F^-). \quad (15)$$

The results for the cobalt fluorides are shown in Table 2. HF results for CoF_3 using the smaller basis sets (basis 4 and basis 5 in Table 2) are missing, as the calculations were unable to preserve the expected degeneracy in the Co 3d orbitals.

4.1 | Intra- vs inter-atomic correlation

While the minimal basis set results (basis 5) do not seem to follow any trend, one can observe the expected decrease, that is, more negative values, in correlation energy for all individual systems with increased basis set size. Except for the largest basis set (basis 1), the interatomic correlation energy ΔE_{corr} follows the same trend. Thus additional basis functions on fluorine allow for more intra-atomic correlations on the fluorine atoms and reduce the amount of interatomic correlation between Co and F. The trend in the interatomic correlation energy (per F atom), however, remains similar for the largest two basis sets (basis 1 and basis 2): The two CoF_4 geometries show very similar values, while CoF_2 has smallest interatomic correlation and CoF_3 represents an intermediate situation. This trend, however, changes when removing AO basis functions on Co (basis 3 and basis 4). In this case, the two CoF_4 interatomic correlation energies start to deviate more. Adding additional basis functions to a minimal basis on Co is thus critical even for a qualitative description of the correlation energy of the different systems. On the other hand, additional basis functions on F mostly yield quantitative improvements, without changing the relative energies much. The very similar correlation energies for both CoF_4 structures also indicate that correlation has only a weak influence on the geometry. In terms of the energy difference

TABLE 1 HF, FCI, and correlation energies (in E_h) for the different cobalt cations and F^- using different basis set

	HF	FCI	E_{corr}
cc-pVDZ [6s,5p,3d,1f]			
Co^{2+}	−1380.596424	−1380.749118	−0.152694
Co^{3+}	−1379.432768	−1379.528192	−0.095423
Co^{4+}	−1377.606402	−1377.653136	−0.046734
cc-pVDZ [3s,2p,1d]			
F^-	−99.365984	−99.558917	−0.192934
Minimal basis + 4sp [4 s,3p,1d]			
Co^{2+}	−1380.532708	−1380.533252	−0.000544
Co^{3+}	−1379.112148	−1379.112396	−0.000248
Co^{4+}	−1376.890476	−1376.890552	−0.000076
Minimal basis + 4s [4s,2p,1d]			
Co^{2+}	−1380.529043	−1380.529126	−0.000083
Co^{3+}	−1379.092596	−1379.092637	−0.000041
Co^{4+}	−1376.846931	−1376.846931	−0.000000

Note: Systems without correlation energy at their minimal basis set are omitted.

TABLE 2 HF, FCI, and correlation energies (in E_h) for the cobalt fluorides using different basis sets

	HF	FCI	E_{corr}	Std. Dev.	ΔE_{corr}	ΔE_{corr} per F
Basis 1: cc-pVDZ (Co [6s,5p,3d,1f], F [3s,2p,1d])						
CoF_2	−1580.389262	−1581.022206	−0.632944[a]	3.2×10^{-5}	−0.094383	−0.047191
CoF_3	−1679.813744	−1680.635657	−0.821913[a]	1.6×10^{-4}	−0.147833	−0.049278
CoF_4 D_{4h}	−1779.019872	−1780.124419	−1.104546[a]	4.9×10^{-4}	−0.286078	−0.071520
CoF_4 T_d	−1779.104549	−1780.211897	−1.107348[a]	6.9×10^{-4}	−0.288879	−0.072220
Basis 2: cc-pVDZ on Co, minimal on F (Co [6 s,5p,3d,1f], F [2s,1p])						
CoF_2	−1580.361724	−1580.678793	−0.317070[a]	4.4×10^{-5}	−0.164375	−0.082188
CoF_3	−1679.770945	−1680.131453	−0.360508[a]	1.1×10^{-4}	−0.265085	−0.088362
CoF_4 D_{4h}	−1778.963170	−1779.455709	−0.492539[a]	1.4×10^{-4}	−0.445805	−0.111451
CoF_4 T_d	−1779.051622	−1779.541594	−0.489973[a]	1.7×10^{-4}	−0.443239	−0.110810
Basis 3: minimal basis + Co 4sp (Co [4s,3p,1d], F [2s,1p])						
CoF_2	−1580.219451	−1580.302693	−0.083241		−0.082697	−0.041349
CoF_3	−1679.512361	−1679.699007	−0.186646		−0.186398	−0.062133
CoF_4 D_{4h}	−1778.753694	−1778.992539	−0.238846		−0.238770	−0.059692
CoF_4 T_d	−1778.806597	−1779.069714	−0.263116		−0.263040	−0.065760
Basis 4: minimal basis + Co 4s (Co [4s,2p,1d], F [2s,1p])						
CoF_2	−1580.118522	−1580.179205	−0.060683		−0.060600	−0.030300
CoF_3						
CoF_4 D_{4h}	−1778.666630	−1778.843568	−0.176939		−0.176939	−0.044235
CoF_4 T_d	−1778.701932	−1778.910543	−0.208612		−0.208612	−0.052153
Basis 5: minimal basis (Co [3s,2p,1d], F [2s,1p])						
CoF_2	−1579.998988	−1580.010936	−0.011948		−0.011948	−0.005974
CoF_3						
CoF_4 D_{4h}	−1778.552226	−1778.788008	−0.235782		−0.235782	−0.058945
CoF_4 T_d	−1778.696523	−1778.845614	−0.149091		−0.149091	−0.037273

Note: Detailed information on all used basis sets is available in the Tables S1 to S6 of Supplementary Information 1.
[a]FCIQMC correlation energy with SD.

between the T_d and D_{4h} structures, HF yields a quantitatively reasonable results in good agreement with the FCIQMC value ($\Delta E^{HF}_{D_{4h}-T_d} = 84.7$ mE_h, $\Delta E^{FCI}_{D_{4h}-T_d} = 87.5$ mE_h).

The effect of gaining more intra-atomic correlation energy when using the larger basis set on F (basis 1) may be confirmed by a QIT analysis of both basis sets (basis 1 vs basis 2), as shown in Tables S7 and S8. The mutual information of orbital pairs including one F 2p AO and one Co AO (eg, orbital pairs #2#5 and #2#6) is smaller using the larger basis set. In contrast, the mutual information between two F orbitals (without Co AO contributions) increases for the larger basis set (eg, #2#37 in the full cc-pVDZ basis, corresponding to #2#28 in the smaller basis set). For isosurface plots of all orbitals, refer to Supplementary Information 2. It should be noted, however, that a direct correspondence between the AO basis set effect and the QIT data is difficult, as the QIT data are based on delocalized MOs while the basis set effects are directly related to AO basis functions.

4.2 | AO mixing for bonding orbitals

Another trend that changes character depending on the AO basis set size is the interatomic correlation energy ΔE_{corr} per F atom of the CoF_3 model (cf. Table 2). For the larger two basis sets (basis 1 and basis 2) it is very close to the CoF_2 value and much smaller than for CoF_4. On the other hand, it is very close to CoF_4 if only the Co 4sp functions are added to the minimal basis set (basis 3). This might be connected to the character of the 3*d* orbitals, which are summarized in Table 3. The numbers represent MO indices and indicate whether the corresponding MO is mostly constituted by a single Co 3*d* AO (single number), or mixed with F 2p AOs (two numbers). For example in CoF_2 the MO with index 4 is almost identical with the $3d_{x^2-y^2}$ AO, while the $3d_{z^2}$ AO contributes mostly to MO 3 and additionally to MO 5 with some smaller contribution.

Thus MOs 3 and 5 may be considered as hybridized. Additionally, these two MOs form a pair of bonding and antibonding orbitals, that is, the latter has an additional nodal plane perpendicular to the Co—F bonding axes. Assignment of the MOs and their AO contributions is based on the isosurface plots (cf. Supplementary Information 2). In the CoF_2 model, the MOs are dominated by Co 3d AO contributions. The minor F 2p contributions in $3d_{z^2}$ may be related to the state-averaged CASSCF(5,7) including the $^4\Sigma_g^-$ as indicated in Figure 2. There the $3d_{z^2}$ orbital is singly occupied and thus gets mixed with other AOs. This needs to be corrected by a CI calculation targeting the $^4\Delta_g$ only. Both CoF_4 models show, in contrast to CoF_2, F 2p contributions in all MOs related to the Co 3d orbitals, while CoF_3 shows a more mixed situation: The $3d_{z^2}$ orbital remains on its own, and the other four 3d orbitals are mixed with varying degrees of F 2p contributions. The mixed MOs would require more flexibility in the AO basis set, especially for the Co 3d orbitals that are highest in energy among the occupied orbitals. The F 2p AOs, however, which are energetically lower and thus are all doubly occupied, are sufficiently described by a smaller basis set. Therefore, the qualitative trend in interatomic correlation energy, which relates to the bonding description, does change when adding more AO basis functions on Co, but not on F. The much smaller value for CoF_2 however is already visible for smaller basis sets on Co as the 3d orbitals mix much less than for the other three cases.

The Co 3d orbitals and their mixing with the F 2p orbitals may also be interpreted in terms of the bonding situation. In case of AO mixing, the pairs of bonding and antibonding MO yield the largest mutual information of the systems (cf. Tables S7 to S11), which indicates a large and systematic problem of HF in describing these MOs. Correction on the CI level then requires large entanglement of these orbitals. As a result, increasing interatomic correlation energies are observed. In fact, such arguments have been made a long time ago[44–46] and similar observations have been made for N_2.[47] There, the effect increased for large internuclear separations, where strong correlation becomes very important.

4.3 | Comparison of different correlation measures

Largest overall mutual information is observed for CoF_4 D_{4h} ($I^{max}_{77,78} = 0.4066$) and CoF_4 T_d ($I^{max}_{5,7} = 0.2096$), while CoF_3 and CoF_2 show smaller values (cf. Tables S7 to S11). This agrees with the trend of strong correlation as measured by the total correlation I_{tot} (QIT based) and the coupled cluster-based T_1 and D_1 diagnostics, summarized in Table 4. In general, the FCIQMC energies are much smaller than the DMRG results, as the latter is primarily developed for static correlation and thus struggles with the dynamic correlation contribution. FCIQMC on the other hand is able to consider both. The table also includes DMRG results using Pipek-Mezey[48] localized orbitals. As observed earlier, additional basis functions on fluorine reduce interatomic correlations between Co and F, that is, intra-atomic correlations are preferred. This may be exploited by using localized MOs. In turn this requires more mixing of orbitals participating in the chemical bonds. The localized orbitals result in a much lower DMRG

TABLE 3 Mixing of the Co 3d AOs in CoF_n

	$3d_{z^2}$	$3d_{x^2-y^2}$	$3d_{xy}$	$3d_{xz}$	$3d_{yz}$
CoF_2	3, (5)	4	32	48, (50)	54, (56)
CoF_3	6	4, 7	31, 34	66, (65)	52, (50)
CoF_4 D_{4h}	5, (4)	3, 6	50, 52	70, 71	77, 78
CoF_4 T_d	5, 7	75, 77	3, 8	34, 37	55, 58

Note: The numbers indicate the index of the MOs with largest Co 3d AO contributions. A single number indicates the corresponding 3d AO does not mix, while two numbers indicate the Co 3d orbital is hybridized with F 2p orbitals, forming a pair of bonding and anti-bonding orbitals (ie, whether there is a nodal plane perpendicular to the Co–F bonding axes). Numbers in parenthesis indicate only a small Co 3d contribution to the MO. Surface plots of all the MOs are available in the SI.

TABLE 4 Summary of the DMRG results including the total energies and differences to FCIQMC ΔE (units in E_h) as well as the total correlation I_{tot} of the cobalt fluorides

	FCIQMC	RCCSD(T)	DMRG	$\Delta E_{FCI\ -\ DMRG}$	I_{tot}	T_1	D_1
CoF_2 (cc-pVDZ)	−1581.0222	−1581.0159	−1580.8079	−0.2143	3.01	0.032	0.076
CoF_2 (cc-pVDZ, local)			−1580.9866	−0.0357	3.24		
CoF_2 (min. basis on F)	−1580.6788		−1580.5841	−0.0947	2.53		
CoF_3 (cc-pVDZ)	−1680.6357	−1680.6365	−1680.4664	−0.1693	4.11	0.042	0.118
CoF_4 D_{4h} (cc-pVDZ)	−1780.1244	−1780.1324	−1779.7190	−0.4054	5.51	0.070	0.263
CoF_4 T_d (cc-pVDZ)	−1780.2119	−1780.2180	−1779.9149	−0.2970	5.23	0.054	0.163

Note: For CoF_2 DMRG results using Pipek-Mezey localized orbitals are included as well. The last two columns give the T_1 and D_1 diagnostics based on RCCSD(T)/cc-pVDZ calculations.

energy although it used much looser numerical parameters (DBSS DM cutoff 1×10^{-4} vs 1×10^{-5}). The obtained MPS for the localized orbitals is thus much more compact and exact. Additionally, the total correlation I_{tot} increased, that is, overall more entanglement is included.

The CoF_4 DMRG calculations for the T_d structure are closer to the FCIQMC energies than for D_{4h} (column $\Delta E_{FCI\ -\ DMRG}$ in Table 4) (note that both systems have very similar FCIQMC correlation energies, cf. E_{corr} for basis 1 in Table 2). At the same time T_d shows slightly less total correlation I_{tot}. Together with the T_1 and D_1 diagnostics that indicate D_{4h} to be more strongly correlated, one would expect DMRG to perform better for D_{4h} than for T_d. Assuming DMRG is indeed able to capture all strong correlation effects, this means the D_{4h} result is missing some important dynamic correlation effects. A possible explanation could be the stronger multireference character in connection with the number of blockstates used. In the less strongly correlated case T_d, only a few configurations directly related to strong correlation generate excited configurations related to dynamic correlation. In D_{4h} on the other hand, more configurations related to strong correlation are required, which in turn generate a larger number of configurations for dynamic correlation. Using the same numerical cutoff parameter for both systems will therefore lead to a different quality and accuracy of the calculation.

The RCCSD(T) energies in Table 4 are in rough agreement with FCIQMC results. While the correlation energy for CoF_2 is underestimated, the CoF_4 energies are overestimated. Following this trend the CoF_3 energies are in very well agreement (less than 1 mE_h), which may therefore be the result of error cancelation.

5 | SUMMARY

In summary, the results suggest a more complete AO basis set on cobalt than for fluorine is required, and intra-atomic are more important than interatomic correlations. Thus the use of localized MOs seems beneficial. The treatment of the extended CoO chains should therefore consider localized orbitals and one may try to reduce the number of basis functions on oxygen/fluorine. The latter suggestion however assumes the results may directly be transferred from fluorine to oxygen and therefore requires careful validation.

ACKNOWLEDGMENTS

Financial support by the International Max Planck Research School "Functional Interfaces in Physics and Chemistry" as well as computing time provided by the high performing computing facilities (ZEDAT) at Freie Universität Berlin is gratefully acknowledged.

AUTHOR CONTRIBUTIONS

Christian Stemmle: Conceptualization; data curation; investigation; methodology; validation; visualization; writing-original draft. **Beate Paulus:** Conceptualization; formal analysis; funding acquisition; supervision; writing-review and editing.

ORCID

Christian Stemmle https://orcid.org/0000-0002-3248-9088

REFERENCES

[1] P.-O. Löwdin, *J. Phys. Chem.* **1957**, *61*, 55.
[2] R. J. Bartlett, *Annu. Rev. Phys. Chem.* **1981**, *32*, 359.
[3] J. D. Watts, J. Gauss, R. J. Bartlett, *J. Chem. Phys.* **1993**, *98*, 8718.
[4] P. G. Szalay, T. Müller, G. Gidofalvi, H. Lischka, R. Shepard, *Chem. Rev.* **2012**, *112*, 108, 22204633.
[5] B. O. Roos, P. R. Taylor, P. E. Siegbahn, *Chem. Phys.* **1980**, *48*, 157.
[6] S. R. White, *Phys. Rev. Lett.* **1992**, *69*, 2863.
[7] G. H. Booth, A. J. W. Thom, A. Alavi, *J. Chem. Phys.* **2009**, *131*, 054106.
[8] J. Hubbard, B. H. Flowers, *Proc. Royal Soc. London. Series A. Math. Phys. Sci.* **1963**, *276*, 238.
[9] M. Motta, D. M. Ceperley, G. K.-L. Chan, J. A. Gomez, E. Gull, S. Guo, C. A. Jiménez-Hoyos, T. N. Lan, J. Li, F. Ma, A. J. Millis, N. V. Prokof'ev, U. Ray, G. E. Scuseria, S. Sorella, E. M. Stoudenmire, Q. Sun, I. S. Tupitsyn, S. R. White, D. Zgid, S. Zhang, *Phys. Rev. X* **2017**, *7*, 031059.
[10] A. V. Sinitskiy, L. Greenman, D. A. Mazziotti, *J. Chem. Phys.* **2010**, *133*, 014104.
[11] L. Veis, A. Antalík, J. Brabec, F. Neese, O. Legeza, J. Pittner, *J. Phys. Chem. Lett.* **2016**, *7*, 4072, 27682626.
[12] S. Wouters, T. Bogaerts, P. Van Der Voort, V. Van Speybroeck, D. Van Neck, *J. Chem. Phys.* **2014**, *140*, 241103.
[13] P. Ferstl, L. Hammer, C. Sobel, M. Gubo, K. Heinz, M. A. Schneider, F. Mittendorfer, J. Redinger, *Phys. Rev. Lett.* **2016**, *117*, 046101.
[14] P. Ferstl, F. Mittendorfer, J. Redinger, M. A. Schneider, L. Hammer, *Phys. Rev. B* **2017**, *96*, 085407.
[15] J. V. Rau, S. Nunziante Cesaro, N. S. Chilingarov, G. Balducci, *Inorg. Chem.* **1999**, *38*, 5695.
[16] M. Korobov, L. Savinova, L. Sidorov, *J. Chem. Thermodyn.* **1993**, *25*, 1161.
[17] T. Schlöder, *Matrix Isolation and Quantum-chemical Study of Molecules containing Transition Metals in High Oxidation States*, Ph.D. thesis, Albert-Ludwigs-Universität Freiburg (**2013**).
[18] V. V. Sliznev, N. Vogt, J. Vogt, *Mol. Phys.* **2004**, *102*, 1767.
[19] J. H. Yates, R. M. Pitzer, *J. Chem. Phys.* **1979**, *70*, 4049.

[20] A. Popovic, A. Lesar, J. V. Rau, L. Bencze, *Rapid Commun. Mass Spectrom.* **2001**, *15*, 749.
[21] R. Fowler, W. Buford III., J. Hamilton Jr., R. Sweet, C. Weber, J. Kasper, I. Litant, *Indus. Eng. Chem.* **1947**, *39*, 292.
[22] S. Riedel, M. Kaupp, *Coord. Chem. Rev.* **2009**, *253*, 606.
[23] R. Horodecki, P. Horodecki, M. Horodecki, K. Horodecki, *Rev. Mod. Phys.* **2009**, *81*, 865.
[24] O. Legeza, R. Noack, J. Sólyom, L. Tincani, in *Computational Many-Particle Physics*, Lecture Notes in Physics, Vol. 739 (Eds: H. Fehske, R. Schneider, A. Weiße), Springer Berlin Heidelberg, **2008**, p. 653.
[25] K. H. Marti, M. Reiher, *Mol. Phys.* **2010**, *108*, 501.
[26] Y. Kurashige, G. K.-L. Chan, T. Yanai, *Nat. Chem.* **2013**, *5*, 660.
[27] S. Z. Szalay, M. Pfeffer, V. Murg, G. Barcza, F. Verstraete, R. Schneider, Ö. Legeza, *Int. J. Quantum Chem.* **2015**, *115*, 1342.
[28] R. Olivares-Amaya, W. Hu, N. Nakatani, S. Sharma, J. Yang, G. K.-L. Chan, *J. Chem. Phys.* **2015**, *142*, 034102.
[29] S. Wouters, C. A. Jiménez-Hoyos, Q. Sun, G. K.-L. Chan, *J. Chem. Theor. Comp.* **2016**, *12*, 2706.
[30] O. Legeza, J. Röder, B. A. Hess, *Phys. Rev. B* **2003**, *67*, 125114.
[31] O. Legeza, J. Sólyom, *Phys. Rev. B* **2004**, *70*, 205118.
[32] O. Legeza, J. Sólyom, *Phys. Rev. B* **2003**, *68*, 195116.
[33] F. R. Petruzielo, A. A. Holmes, H. J. Changlani, M. P. Nightingale, C. J. Umrigar, *Phys. Rev. Lett.* **2012**, *109*, 230201.
[34] N. S. Blunt, S. D. Smart, J. A. F. Kersten, J. S. Spencer, G. H. Booth, A. Alavi, *J. Chem. Phys.* **2015**, *142*, 184107.
[35] D. Cleland, G. H. Booth, A. Alavi, *J. Chem. Phys.* **2010**, *132*, 041103.
[36] G. H. Booth, D. Cleland, A. J. W. Thom, A. Alavi, *J. Chem. Phys.* **2011**, *135*, 084104.
[37] NECI, https://github.com/ghb24/NECI_STABLE.
[38] R. A. Kendall, T. H. Dunning, R. J. Harrison, *J. Chem. Phys.* **1992**, *96*, 6796.
[39] H.-J. Werner, P. J. Knowles, G. Knizia, F. R. Manby, M. Schütz, P. Celani, W. Györffy, D. Kats, T. Korona, R. Lindh, A. Mitrushenkov, G. Rauhut, K. R. Shamasundar, T. B. Adler, R. D. Amos, A. Bernhardsson, A. Berning, D. L. Cooper, M. J. O. Deegan, A. J. Dobbyn, F. Eckert, E. Goll, C. Hampel, A. Hesselmann, G. Hetzer, T. Hrenar, G. Jansen, C. Köppl, Y. Liu, A. W. Lloyd, R. A. Mata, A. J. May, S. J. McNicholas, W. Meyer, M. E. Mura, A. Nicklass, D. P. O'Neill, P. Palmieri, D. Peng, K. Pflüger, R. Pitzer, M. Reiher, T. Shiozaki, H. Stoll, A. J. Stone, R. Tarroni, T. Thorsteinsson, and M. Wang, "Molpro, version 2015.1, a package of ab initio programs," (**2015**), see http://www.molpro.net
[40] H.-J. Werner, P. J. Knowles, G. Knizia, F. R. Manby, M. Schütz, *WIREs Comput. Mol. Sci.* **2012**, *2*, 242.
[41] P. J. Knowles, N. C. Handy, *Chem. Phys. Lett.* **1984**, *111*, 315.
[42] P. J. Knowles, N. C. Handy, *Comput. Phys. Commun.* **1989**, *54*, 75.
[43] O. Legeza, "Qc-dmrg-budapest, a program for quantum chemical dmrg calculations," HAS RISSPO Budapest (**2000**-2016).
[44] S. Diner, J. P. Malrieu, P. Claverie, *Theor. Chim. Acta* **1969**, *13*, 1.
[45] O. Sinanoğlu, Many-electron theory of atoms, molecules and their interactions. in *Advances in Chemical Physics*, John Wiley & Sons, Ltd, **1964**, p. 315.
[46] R. K. Nesbet, Electronic correlation in atoms and molecules. in *Advances in Chemical Physics*, John Wiley & Sons, Ltd, **1965**, p. 321.
[47] C. Stemmle, B. Paulus, O. Legeza, *Phys. Rev. A* **2018**, *97*, 022505.
[48] J. Pipek, P. G. Mezey, *J. Chem. Phys.* **1989**, *90*, 4916.

SUPPORTING INFORMATION

Additional supporting information may be found online in the Supporting Information section at the end of this article.

How to cite this article: Stemmle C, Paulus B. Electron correlation effects in cobalt fluorides CoF_n. *Int J Quantum Chem.* 2020;120: e26203. https://doi.org/10.1002/qua.26203